CESR-C: PERFORMANCE OF A WIGGLER-DOMINATED STORAGE RING*

A.Temnykh# for CESR Operations Group, Cornell University, Ithaca, NY 14850, U.S.A.

INTRODUCTION

Until August 2003, CESR was operating as a electron-positron collider at 5.3 GeV/beam energy providing luminosity at Y resonances. In parallel, Cornell High Energy Synchrotron Source (CHESS) laboratory used synchrotron radiation in parasitic regime. In 2001 we decided to extend CESR operating range to low 1.5 GeV/beam energy. To provide adequate damping at low energy, we designed, fabricated and during two shut downs in 2003 and in 2004 installed 12 super-ferric wiggler magnets [1]. Now CESR operates 60% of time as electron-positron collider at 1.88 GeV/beam energy and the rest 40% as synchrotron radiation source at 5.3 GeV/beam energy.

This paper discusses low energy regime called CESR-c. CESR-c beam parameters presented in Table 1 show absolute domination of the wiggler magnets in radiation damping, in forming horizontal beam emittance, beam energy spread and machine vertical octupole-like nonlinearity.

In the first part of paper we discuss issues linked to damping rings. Here are presented results of verification of beam parameters formed by wigglers, the wigglers magnetic field non-linearity testing and result of the CESR-c dynamic aperture tracking study. The second part describes CESR-c operation as an electron-positron collider. Here we report luminosity and beam-beam interaction performance, present recent results of beam dynamics studies and discuss our improvement plan.

Table 1: CESR-c beam parameters

	No wigglers	With wigglers
Hor. emittance [nm-rad]	30	220
Damping time [ms]	570	55
Energy spread [σ_e/E]	2 x 10^{-4}	8 x 10^{-4}
Vertical non-linearity, dQy/dJy [1/(mm-rad)]	-0.28	3.0

BEAM PARAMETERS AND WIGGLER MAGNET FIELD VARIFICATION

In experiments reported below we verified beam energy spread and characterized the magnetic field of the wigglers using beam based measurements.

Bunch Length and Beam Energy Spread

In optics HIBETAINJ_20040628, with 2.1 T peak field in 12 wigglers and 6 MV of total accelerating RF field, we measured bunch length, σ_z, to be 12 mm. Beam energy spread was calculated from the expression given in [2]:

$$\frac{\sigma_E}{E} = \frac{2\pi f_S}{c|\eta|}\sigma_z$$

Where c is speed of light, η - momentum compaction factor and f_s – synchrotron tune. For CESR-c parameters f_s = 39.2 kHz and η = 0.011 it gives σ_E/E = 8.6x10^{-4} which is very close to the predicted 8.5x10^{-4}. Because the radiation in wigglers dominates over radiation in the rest of the ring, the fact of good agreement between measured and calculated spread means good consistency between wiggler model and real magnet.

Beam Based Wiggler Field Characterization and Model Benchmarking

The first CESR-c wiggler prototype was built and installed in the ring for beam testing in summer 2002. Magnetic field measurements [3] had indicated the presence of a skew-quadrupole moment ~1.5 Gm/cm in this magnet. Later we found the cause of this error [4] and in the later production magnets we corrected this problem. Measurement of the beam coupling [5] in optics with prototype magnet, see Fig. 1, revealed a significant coupling amplitude. The wave analysis [6] indicated the source of the coupling in location of the prototype. The skew-quad moment of the source, ~2.0 Gm/cm, consistent with the field measurement.

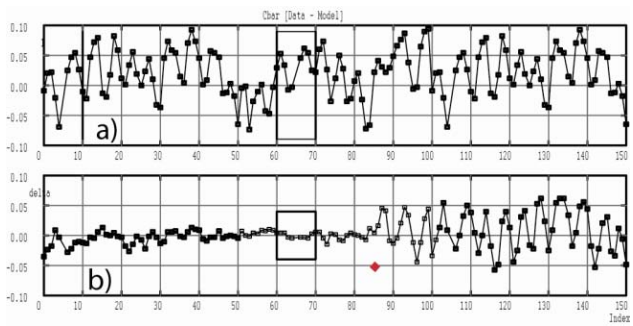

Figure 1: CESR-c coupling measurement. One wiggler optics with 2.1T peak field, Oct 1 2002. The wiggler prototype location is marked by diamond. a) Parameter C12 along the ring, b) wave analysis indicating the coupling source at the wiggler location.

* Work supported by the National Science Foundation
# e-mail: abt6@cornell.edu

In the production wigglers, operating in storage ring now, skew-quadrupole moment is much smaller. The measurements see Fig. 2, indicate that the coupling they generate is negligible.

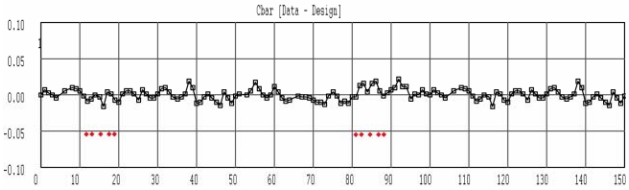

Figure 2: CESR-c coupling measurement. 12 wigglers optics with 2.1T peak field, Oct 11 2004. The wiggler locations are marked by diamonds. C12 data indicate negligible coupling.

In the calculation of beam properties presented below, we used the ring model based on the BMAD subroutine library described in [7]. The model incorporates a third order Taylor map based on an analytical fit to a 3D calculated magnetic field table [8].

One type of experiment characterizing wiggler field was the measurement of betatron tune as a function of the wiggler current. The tune dependence on current is the result of a linear focusing effect of the wiggler field. In experiment we varied the 14WA wiggler current and measured vertical and horizontal tune. The result in comparison with model is given in Fig.3. In calculation we used formulas derived from [9] and field characteristics from 3D magnetic field calculation. A linear fit for vertical tune variation gives dQ_v/dI = 1.15×10^{-3} A^{-1} which is close to the prediction of 1.02×10^{-3}.

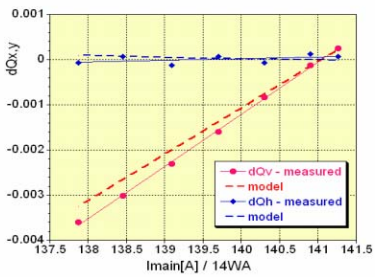

Figure 3: Measured and calculated dependence of tune on current of 14WA wiggler.

The weak dependence of horizontal tune indicated by model, dQ_x/dI = - 3.0×10^{-5} A^{-1}, was also confirmed in experiment, (3.0 ±2.5) x 10^{-5}.

Nonlinear properties of the wiggler field were tested by measuring betatron tune as a function of beam position the wigglers. One example is given in Fig. 4. In this experiment we tested a group of 3 wiggler magnets at 18E location. For vertical and horizontal beam displacement we used localized orbit distortions. All nonlinear magnetic elements in the region of the distortion were turned off. Data in Fig. 4a show strong quadratic dependence of vertical tune and much weaker dependence of horizontal on vertical beam position. Both are in good agreement with calculation. The strong dependence of vertical tune on vertical position is a well known effect. It is caused by interference between beam trajectory wiggling in horizontal plane and longitudinal magnetic field component seen by particles displaced vertically from the wiggler middle plane.

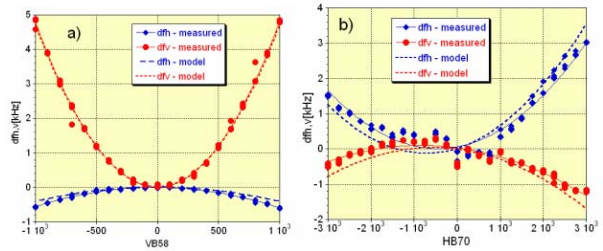

Figure 4: Vertical (circles) and horizontal (diamonds) betatron tune as a function of vertical, a), and horizontal, b), beam position in 18E wiggler cluster, group of 3 wigglers. Modeled dependence is given by dashed line. Vertical scale is 1kHz or 0.025 per division, horizontal 0.5mm/div for a) and 1mm/div for b).

Tune variation with horizontal beam position, see Fig. 4b, is smaller. This variation comes from non-uniformity of magnetic field across wiggler poles and is also in good agreement with calculation. Data collected from other wigglers during testing showed similar consistency with the model predictions.

The dependence of betatron tune on betatron amplitude in storage rings plays a critical role in beam dynamics. It may affect dynamic aperture, nonlinear resonance strength [9], beam-beam interaction performance, [10] etc. Because we are using the model for beam dynamics simulation, it was extremely important to verify consistency between model and machine.

The dependence of betatron tune on betatron amplitude was measured in the following way.

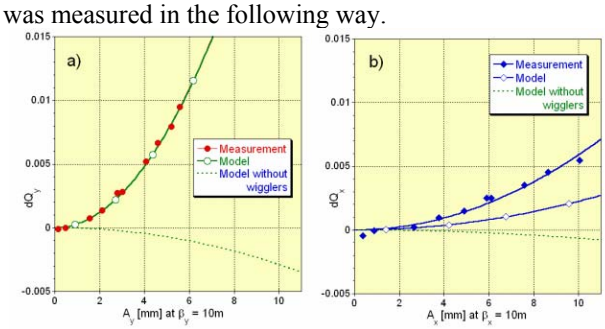

Figure 5: Dependence of vertical, a), and horizontal, b), tune on vertical and horizontal amplitude. Solid points are the measured data, open points mark model calculation, dashed line shows the calculated model without wigglers.

Coherent betatron oscillations in the vertical or horizontal plane were excited by resonant shaking. The resonance condition was maintained by a feedback loop keeping constant phase between beam oscillation and shaking by controlling the driving generator. The amplitude of beam betatron oscillation we controlled by the shaking strength. In the process of data taking, we measured the amplitude of coherent beam oscillation using beam position monitors and driving generator

frequency (equal to betatron tune). Several measurements were made with varying shaking amplitudes.

Fig. 5 depicts the result. Plots "a)" and "b)"present vertical and horizontal tune variation with amplitude. Note that the abscissa scale is the betatron amplitude in mm projected in location with $\beta_{x,y}$ = 10m. A quadratic fit of the data for vertical tune dependence, $dQ_y = C_{yy} * A^2_y$, gives C_{yy} = (3.05 +- 0.04) x 10^{-4} 1/mm^2, which is well consistent with the model predicted 3.01 x 10^{-4}. Without wigglers, model gives C_{yy} ~10 times less. A quadratic fit of horizontal tune data indicates C_{xx} = (5.9 +- 0.2) x 10^{-5} 1/mm^2, while the prediction is 2.2 x 10^{-5} 1/mm^2. The difference between measurement and prediction, dC_{xx} = 3.7 x 10^{-5} 1/mm^2, can be attributed to some uncertainty in the octupole moments of magnetic elements around ring. This difference is only ~10% of nonlinearity observed in vertical plane.

All the above comparisons between experimental data and calculation show a rather good agreement. That establishes the validity of the model. One important tracking result is given in Fig. 6. Here, the plots show CESR-c dynamic aperture scaled to the IP. Marked counters represent maximum amplitude of betatron oscillation in horizontal and vertical plane for particles survived 1000 turns and started with dE/E = 0, 0.003 and 0.006.

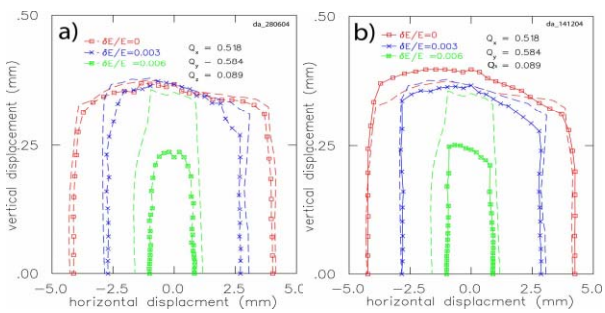

Figure 6: CESR-c dynamic (marked lines) and "mechanical" (dashed lines) aperture obtained with tracking. a) optics with nonlinear wiggler model, b) optics with linearized wigglers. Other details are in text.

All tracking includes the mechanical aperture limitation given by the beam pipe. Dashed lines are for maximum amplitudes of particles surving only 20 turns. These lines give an idea about "mechanical" aperture. Plot "a)" is for optics with nonlinear wiggler model and plot "b)" is for the case when non-linear components were removed from the wiggler model. Comparing these plots one can see only minor differences; i.e., CESR-c dynamic aperture is negligibly affected by the wiggler nonlinearity.

Concluding this section we can state that the good consistency between beam-based wiggler magnetic field characterization and the model prediction validates our wiggler and whole ring models, and indicates the satisfactory quality of the CESR-c wiggler magnets.

CESR-C PRESENT STATUS

In this section we review CESR-c up to date performance, describe operation, present, as example, one result of beam dynamic study and discuss improvement plane.

Table 2: CESR-c machine parameters

Beam current e+/e- [mA]	90 / 70
Number of bunches	40
Synchrotron tune, ν_s	0.1
Bunch length [mm]	11.9
β_y / β_x at IP [m]	0.011 / 0.87
Vertical BB tune shift $\xi_y(+)$ / $\xi_y(-)$	~ 0.035 / ~0.019
Horizontal BB tune shift $\xi_x(+)$ / $\xi_x(-)$	~ 0.025 / ~0.030
Luminosity 10^{32} [1/cm^2/sec]	0.62

CESR-c performance and operation

In the final configuration with all 12 wigglers installed, CESR-c operated for about 6 months. This time was devoted to machine studies (25%), luminosity running (66%) and maintenance shut downs (4%). The average down time due to various systems failing was around 5%. The machine performance as of April 4 2005, end of the recent CESR-c running period, is shown in Table 2.
An example of the beam current and luminosity over 12 hour period running are shown in Fig. 7.

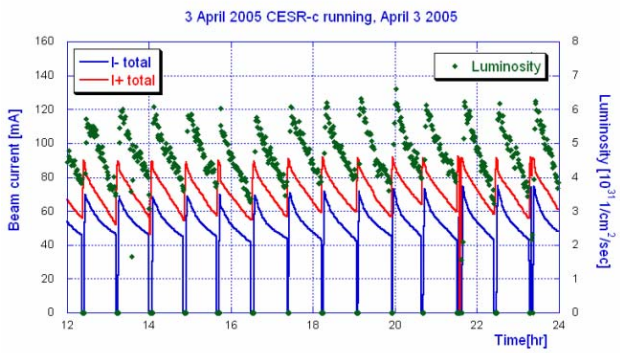

Figure 7: Luminosity and beam current during a 12 hour period.

Here one can see 90mA of maximum positron and 70mA of electron beam current. The positron beam current is very close to the long range beam-beam interaction limit. For large positron current, electron beam life time became short even if beams are not in collision. The electron beam current was empirically optimized for maximum integrated luminosity.

Figures 8 and 9 depict vertical beam size measured in arcs and projected to the IP and vertical beam-beam tune shift parameters calculated from the beam current and beam size.

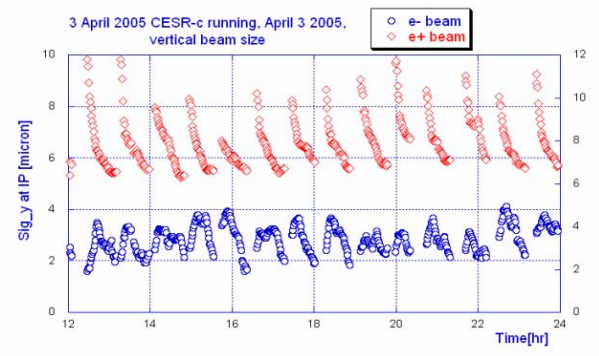

Figure 8: Vertical beam size at IP.

The data in Fig. 8 indicate that at IP electron and positron beams have very different vertical size. The positron beam in average is 2 times larger. This difference is caused by beam-beam interaction. In non-colliding state both beams have approximately equal size of 2.4 microns. The mismatch between electron and positron beam size causes ~50% of luminosity losses. The unequal vertical beam size results in the difference in vertical beam-beam tune shift parameter ξ_y for electron and positron beam seen in Fig. 9.

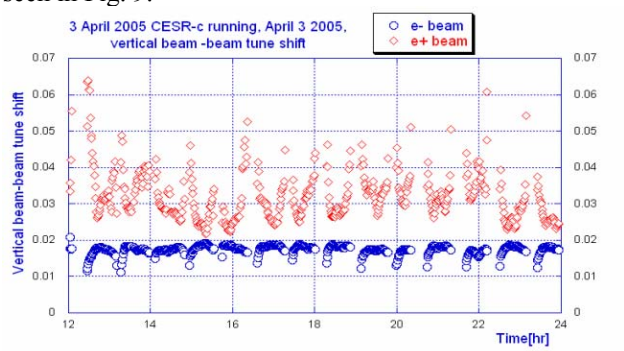

Figure 9: Vertical beam-beam tune shift parameter.

While ξ_y for the positron beam reaches 0.035-0.040, for the electron beam it is below 0.02. Horizontal beam-beam tune shift is around 0.030 for electron beam and 0.025 for positron, primarily from the difference in beam currents.

By changing coupling or betatron tunes electron and positron beam sizes can be easily flopped, indicating the presence of flip-flop phenomena similar to that observed in PEP-II [11].

A detailed simulation with beam-beam interaction and full treatment of lattice nonlinearities suggests that a significant loss in luminosity comes from the energy dependence of the compensation of the experimental solenoid field [12]. The same simulation technique suggests that a 50% increase in luminosity may be obtained by using anti-solenoid compensation similar to that used in the DAFNE storage rings [13].

CESR-c beam dynamics: 2fh – fs = f0 resonance damping

During machine studies period significant efforts were devoted to CESR-c beam dynamics study. One result is presented below.

In the luminosity simulation and later in experiments we found the optimal working point location to be in a region close to the half integer resonance in vicinity of fh ~ 205kHz, fv ~ 235kHz. The CESR revolution frequency, f0, is 390kHz, so in fractional tune units it is Qx ~ 0.525, Qy ~ 0.603.

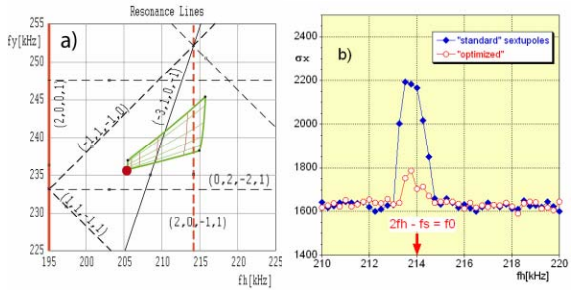

Figure 10: a) Tune plane with resonance lines in vicinity of CESR-c working point (solid circle). Beam-beam tune spread "footprint" corresponds to $\xi_x = 0.025$, $\xi_y = 0.025$. b) Single (non-colliding) beam tune scan. Horizontal beam size as function of horizontal tune when working point crosses resonance 2fh – fs = f0. Solid points mark data with "standard" sextupole distribution, open are for "optimized".

When we vary the working point in that region we found a very strong resonance causing beam loss. The resonance was identified as 2fh – fs =f0. On plot "a)" in Fig. 10, it is marked as (2, 0, -1, 1). Analytically and with tracking we established that this resonance is driven by sextupole magnets sited in locations with dispersion. Later we developed an algorithm for the design of sextupole distribution which does not drive this resonance. However, when we loaded the designed sextupoles into machine we found a significant reduction of resonance strength, but it was still noticeable in horizontal beam size and in beam life time when directly on resonance. To damp the resonance completely we had to do "fine" sextupole tuning. The effect of this is shown on plot "b)" in Fig. 10. Two data sets show the measured horizontal beam size of a single beam as function of horizontal tune for "standard" sextupoles and for "optimized". The difference is in 4 magnets, 10W/E sextupoles differ by -0.050 $1/m^2$ and 24W/E sextupoles by 0.004 $1/m^2$. The "fine" tuning resulted in 4 times reduction of resonance strength.

Fig. 11 presents the data indicating a strong effect of the resonance excitation on beam-beam performance. In this experiment we used two single bunch beams with 2 mA/bunch current. Plot "a)" shows the horizontal spectrum non-colliding beams (dashed line) and two spectra of colliding beams in optics with "standard" (open marks) sextupoles and "optimized" (solid marks) when resonance was damped. While non-colliding beams have a narrow single peak, the colliding beams spectrum is much wider and displays two peaks called "σ" and "π" modes. Between these, there is another peak corresponding to the 2fh – fs =f0 resonance. The amplitude of this peak is much smaller for optimized sextupoles. We interpret this as the following. The beam-

beam interaction spreads the tune of the particles from the working point to higher values as is shown by the beam-beam "footprint" in Fig. 10. Some of them get into resonance at 2fh-fs=f0. These particles are responsible for the resonance peak seen in colliding beam spectrum. In optics with "optimized" sextupoles, the resonance is weaker, the number of particles in resonance lesser and the peak is smaller. One can also notice that the resonance damping shifts the "π" mode higher, implying higher beam density in the beam center and higher luminosity.

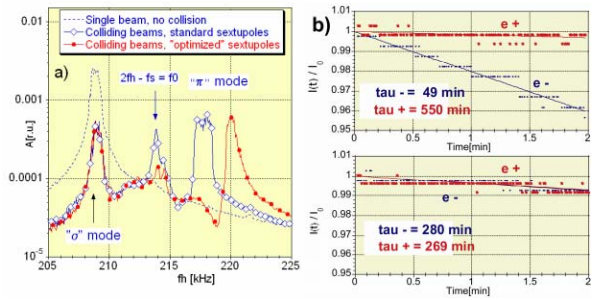

Figure 11: a) Horizontal spectrum of a non-colliding beams, dashed line, and beams in collision with "standard" sextupoles (open marks) and "optimized" sextupoles (solid marks), b) colliding beam current as a function of time for "standard" (upper) and "optimized" (lower plot) sextupoles, resonance damped.

Plot "b)" in Fig. 11 shows the effect of 2fh – fs = f0 resonance damping on colliding beam life time. It presents colliding beam currents as a function of time for "standard" sextupoles and "optimized". The slope indicates the beam loss rate which is inverse proportional to life time. One can see when resonance was damped electron beam life time was approximately 5 times longer.

IMPROVEMENT PLAN

We will improve CESR-c luminosity and operation efficiency persuading the following:

- Continue extensive machine study. Better understanding of the beam dynamics certainly will help us solve many problems.
- Develop new and upgrade the existing beam instrumentation, see for example [14]. This will simplify machine tuning and will reduce the negative effect of transitions between CHESS and CESR-c operation modes.
- Injection into collision will improve peak to average luminosity ratio and, probably, lead us to better beam-beam performance.
- Upgrade of CLEO solenoid compensation scheme as it was mentioned above.

CONCLUSION

During the first 6 month period of CESR-c operation we collected 182 Pb^{-1} of integrated luminosity, verified properties of super-conducting wiggler magnets, developed new beam instrumentations, explored specific for CESR-c aspects of beam dynamics and made progress in luminosity tuning. We found the effects limiting CESR-c luminosity are:

- Beam-beam interaction at IP
- Machine performance such as electron/positron beams differential coupling, non-linear resonances driven by machine nonlinear elements and etc.

The plan for improvement addresses all these issues.

ACKNOWLEDGEMENT

Author would like to thank CESR operating group for a great cooperation and help in data collection. Author is especially grateful to David Rice and David Rubin for encouraging discussions and help in the report preparation.

REFERENCES

[1] D. Rice, S. Chapman et all, "Production and Testing Consideration for CESR-c Wiggler Magnets" PAC'03, Portland, May 2003, p. 167.
[2] A. Chao and M. Tigner, "Handbook of Accelerator Physics and Engineering", p. 187.
[3] A. Temnykh, "Vibrating Wire and Flipping Coil Magnetic Measurement of a CERS-c 7-pole Wiggler Magner", PAC'03, Portland, May 2003, p. 1026.
[4] A. Temnykh, "CESR-c Wiggler & Beam Measurement", Presentation on WIGGLE05 Workshop, Frascati Feb. 2005. Web site: http://www.lnf.infn.it/conference/wiggle2005/talks/Temnyk.pdf
[5] P. Bagley and D. Rubin, "Correction of Transverse Coupling in a Storage Ring" PAC'89, Chicago, March 1989, p.1837
[6] D. Sagan, "Betatron phase and coupling correction at the Cornell Electron/Positron Storage Ring", Phys. Rev. ST Accel. Beams 3, 102801 (2000).
[7] D. Sagan, http://www.lns.cornell.edu/~dcs/bmad
[8] D.Sagan et al., "ICFA Beam Dynamics Newletters 31, 2003" p.48
[9] H. Wiedemann, "Particle Accelerator Physics II," Springer-Verlag, Berlin, Heidelberg (1995).
[10] A. Temnykh, "Influence of the Qubic Nonlinearity of Guiding Magnetic Field on Beam-Beam Interaction in VEPP-4 Storage Ring", XIII International Conference on High Energy Accelerators, Novosibirsk, Aug. 1986, p. 78.
[11] R. L. Holtzapple et al., "Observation of Beam Size Flip-Flop in PEP-II", EPAC 2002, Paris, France, June 2002, p. 410.
[12] D. Rubin, "CLEO solenoid compensation effect" February 7 and March 7, 2005. Internal reports
[13] D. Rubin et al., "CLEO solenoid compensation effect" March 7, 2005. Internal reports
[14] M.Palmer et al., "Design and Operation of a Radiative BhaBha Luminosity Monitor for CESR", RPAT062 this conference.